Mammalian cell proliferation requires noncatalytic functions of O-GlcNAc transferase

Zebulon G. Levine[a], Sarah C. Potter[a], Cassandra M. Joiner[b], George Q. Fei[a], Behnam Nabet[c,d], Matthew Sonnett[e], Natasha E. Zachara[f], Nathanael S. Gray[c,d], Joao A. Paulo[g], and Suzanne Walker[a,1]

[a]Department of Microbiology, Blavatnik Institute of Harvard Medical School, Boston, MA 02115; [b]Department of Chemistry, St. Olaf College, Northfield, MN 55057; [c]Department of Cancer Biology, Dana-Farber Cancer Institute, Boston, MA 02115; [d]Department of Biological Chemistry and Molecular Pharmacology, Blavatnik Institute of Harvard Medical School, Boston, MA 02115; [e]Department of Systems Biology, Blavatnik Institute of Harvard Medical School, Boston, MA 02115; [f]Department of Biological Chemistry, Johns Hopkins University School of Medicine, Baltimore, MD 21205; and [g]Department of Cell Biology, Blavatnik Institute of Harvard Medical School, Boston, MA 02115

This contribution is part of the special series of Inaugural Articles by members of the National Academy of Sciences elected in 2020.

Contributed by Suzanne Walker, November 19, 2020 (sent for review August 7, 2020; reviewed by Benjamin F. Cravatt and Matthew R. Pratt)

O-GlcNAc transferase (OGT), found in the nucleus and cytoplasm of all mammalian cell types, is essential for cell proliferation. Why OGT is required for cell growth is not known. OGT performs two enzymatic reactions in the same active site. In one, it glycosylates thousands of different proteins, and in the other, it proteolytically cleaves another essential protein involved in gene expression. Deconvoluting OGT's myriad cellular roles has been challenging because genetic deletion is lethal; complementation methods have not been established. Here, we developed approaches to replace endogenous OGT with separation-of-function variants to investigate the importance of OGT's enzymatic activities for cell viability. Using genetic complementation, we found that OGT's glycosyltransferase function is required for cell growth but its protease function is dispensable. We next used complementation to construct a cell line with degron-tagged wild-type OGT. When OGT was degraded to very low levels, cells stopped proliferating but remained viable. Adding back catalytically inactive OGT rescued growth. Therefore, OGT has an essential noncatalytic role that is necessary for cell proliferation. By developing a method to quantify how OGT's catalytic and noncatalytic activities affect protein abundance, we found that OGT's noncatalytic functions often affect different proteins from its catalytic functions. Proteins involved in oxidative phosphorylation and the actin cytoskeleton were especially impacted by the noncatalytic functions. We conclude that OGT integrates both catalytic and noncatalytic functions to control cell physiology.

O-GlcNAc transferase | OGT | HCF-1 | enzyme | cell proliferation

O-linked *N*-acetylglucosamine transferase (OGT) is the most conserved glycosyltransferase encoded in the human genome (Fig. 1*D* and *SI Appendix*, Fig. S1*A*) (1, 2) and is essential for mammalian cell survival (3–5). Unlike other glycosyltransferases, which act in the endoplasmic reticulum and Golgi apparatus, OGT is found in the nucleus, cytoplasm, and mitochondria (6, 7). OGT attaches the monosaccharide O-linked *N*-acetylglucosamine (O-GlcNAc) to serine and threonine side chains of thousands of proteins (Fig. 1*A*) (6, 8). O-GlcNAc modifications are often dynamic and can be removed by the glycosidase O-GlcNAcase (OGA) (6, 9, 10). Because protein O-GlcNAc levels are sensitive to nutrient conditions and are cytoprotective against multiple forms of cellular stress, the modification is thought to be important in maintaining cellular homeostasis (6, 11–13). High O-GlcNAc levels correlate with aggressiveness for multiple forms of cancer (14–17), and have been implicated in the pathogenesis of metabolic syndrome. It is therefore speculated that inhibiting OGT's catalytic activity will lead to therapeutic benefit for treating cancer or cardiometabolic disease (8, 18–21).

OGT is essential for cell viability and impacts numerous aspects of cell physiology, including metabolism, gene expression, and cell signaling. Its broad effects have been attributed to its widespread Ser/Thr glycosylation activity (8, 22, 23), yet OGT has other biochemical functions that may be important for viability. In an unusual example of a physiologically relevant second enzymatic activity that occurs in the same active site, OGT proteolytically cleaves the essential transcriptional coregulator HCF-1 (Fig. 1*B* and *SI Appendix*, Fig. S1*B*) (24–26); this proteolytic maturation process is proposed to be critical for cytokinesis (26–29). In addition to catalyzing both glycosylation and cleavage reactions, OGT interacts with binding partners (Fig. 1*C*) that recruit OGT to specific substrates (3, 30–34). Recent evidence suggests OGT can regulate *Caenorhabditis elegans* physiology independently of its catalytic functions (35, 36); however, given that OGT is not essential in *C. elegans* (37), it remains unclear whether OGT's binding interactions are essential as well as whether they broadly regulate mammalian physiology independent of OGT's enzymatic activity (38, 39).

Significance

Mammalian cells contain only one glycosyltransferase, OGT, that operates in the nucleus and cytoplasm rather than the secretory pathway. OGT is required for cell proliferation, but a basic unanswered question is which OGT functions are essential. This question is challenging to address because OGT has thousands of glycosylation substrates, two different enzymatic activities, and a large number of binding partners. Here, by establishing genetic tools to replace endogenous OGT with variants that preserve only a subset of its activities, we show that only a low level of glycosylation activity is required to maintain cell viability; however, cell proliferation requires noncatalytic OGT function(s). The ability to replace OGT with variants provides a path to identifying its essential substrates and binding partners.

Author contributions: Z.G.L., J.A.P., and S.W. designed research; Z.G.L., S.C.P., C.M.J., G.Q.F., and J.A.P. performed research; Z.G.L., B.N., N.E.Z., and N.S.G. contributed new reagents/analytic tools; Z.G.L., M.S., and J.A.P. analyzed data; and Z.G.L., S.C.P., and S.W. wrote the paper.

Reviewers: B.F.C., Scripps Research Institute; and M.R.P., University of Southern California.

Competing interest statement: B.N. is an inventor on patent applications related to the dTAG system (WO/2017/024318, WO/2017/024319, WO/2018/148443, and WO/2018/148440). N.S.G. is a scientific founder, member of the Scientific Advisory Board (SAB) and equity holder in C4 Therapeutics, Syros, Soltego, B2S, Gatekeeper, and Petra Pharmaceuticals. The N.S.G. laboratory receives or has received research funding from Novartis, Takeda, Astellas, Taiho, Janssen, Kinogen, Voroni, Her2llc, Deerfield, and Sanofi.

[1]To whom correspondence may be addressed. Email: suzanne_walker@hms.harvard.edu.

This article contains supporting information online at https://www.pnas.org/lookup/suppl/doi:10.1073/pnas.2016778118/-/DCSupplemental.

Published January 8, 2021.

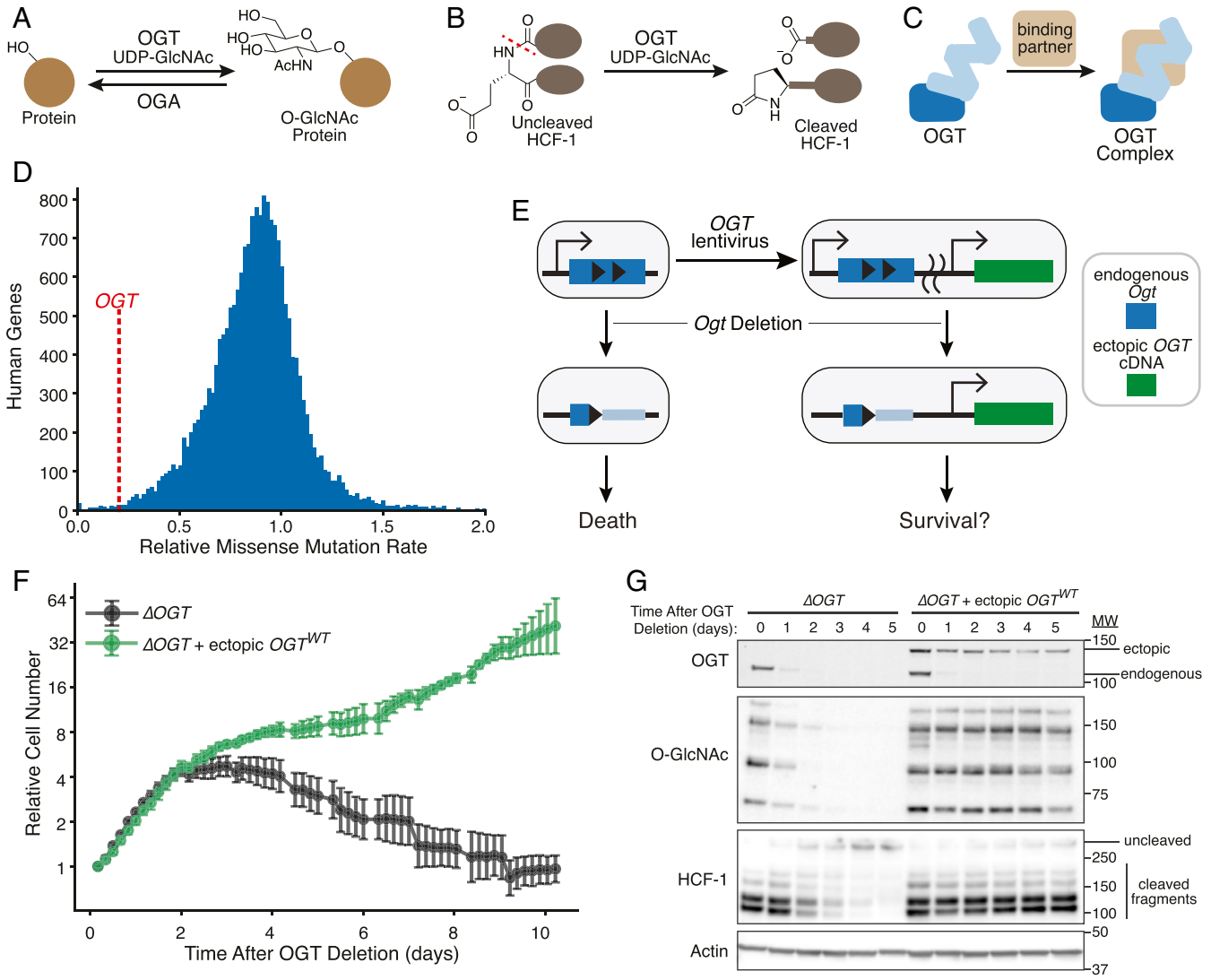

Fig. 1. Ectopic expression of *OGT* complements loss of endogenous gene. (*A*) OGT transfers GlcNAc from UDP-GlcNAc to Ser/Thr residues of many nuclear and cytoplasmic proteins. OGA removes O-GlcNAc. (*B*) OGT cleaves essential transcriptional regulator HCF-1. Glutamate glycosylation-induced peptide backbone rearrangement and cleavage leaves a pyroglutamate on the C-terminal fragment. (*C*) OGT forms multiple protein complexes. (*D*) *OGT* is one of the most conserved human genes. Histogram shows genome-wide amino acid conservation based on a human exome database (2). *OGT* is marked by dashed red line at 0.20. The *x* axis is truncated at 2. (*E*) *OGT* replacement at an ectopic locus can test which OGT features are required for cell survival. Engineered MEFs (40) allow deletion of endogenous *Ogt*. We tested if lentiviral introduction of a single *OGT* isoform could complement defects in cell survival and OGT activity. (*F*) Ectopic *OGT* expression rescues cell growth. Cells with or without ectopic *OGT* were imaged every 4 h after inducing *Ogt* knockout at t = 0. Relative cell number is based on normalized measurements of confluence from live cell imaging. Error bars are SD ($n = 6$ per condition). (*G*) Ectopic *OGT* expression rescues biochemical activities lost upon *Ogt* knockout. Immunoblot analysis shows endogenous and ectopic OGT, protein O-GlcNAc bands (measured by pan-O-GlcNAc monoclonal antibody RL2), and uncleaved HCF-1 or cleaved fragments. See also *SI Appendix*, Fig. S1 *A–F*.

Here we developed a complementation strategy to evaluate whether OGT's catalytic functions are essential for mammalian cell growth. We then modified the strategy to evaluate contributions of OGT's noncatalytic functions to cell proliferation and to link OGT's biochemical activities to the biological pathways they regulate. Our study answers the fundamental question of which of OGT's biochemical activities are needed for cell growth, has implications for how to target OGT in cancer and metabolic disease, and provides tools and approaches that will lead to a better understanding of this unusual protein.

Results

Inducible *OGT* Complementation Rescues Cell Growth. To test which OGT functions are required for cell survival, we developed a complementation system starting from a mouse embryonic fibroblast (MEF) cell line in which Cre-recombinase-mediated *Ogt* knockout is induced by drug treatment (4, 5, 40). Because OGT is normally produced as multiple isoforms (8), we first tested whether a single isoform could rescue knockout of endogenous *Ogt* (Fig. 1*E*). We infected MEFs with a lentiviral vector (41) encoding human OGT, which has 99.8% amino acid identity with that of mouse OGT. Human OGT was produced as a fusion to the red fluorescent protein mKate2; FACS-based selection of cells with sufficient ectopic OGT levels corrected for variable transgene expression due to stochastic lentiviral genomic integration (*SI Appendix*, Fig. S1 *C* and *D*) (42, 43). To test for complementation, we tracked cell abundance by live cell imaging after knocking out the endogenous *Ogt* copy. As expected (40), cells without *Ogt* underwent growth arrest at 2 d and died over the subsequent week (Fig. 1*F* and *SI Appendix*, Fig. S1*E*).

Cells lacking endogenous *Ogt* but harboring ectopic human *OGT* continued to grow, showing that a single OGT isoform can rescue growth (Fig. 1*F*).

Immunoblot analysis of relevant biomarkers confirmed that genetic complementation maintained OGT's catalytic activities (Fig. 1*G*). OGT produced from the endogenous gene (Fig. 1*G*, OGT, *Lower* band) became undetectable 2 d after knockout, and in the absence of ectopic *OGT*, we observed loss of protein O-GlcNAc bands and accumulation of uncleaved HCF-1. OGA synthesis, which is down-regulated by low protein O-GlcNAc levels (40, 44), greatly decreased without OGT (*SI Appendix*, Fig. S1*F*). By day 3, we observed a 42-kDa PARP-1 fragment associated with necrosis (*SI Appendix*, Fig. S1*F*) (45, 46). However, in cells producing mKate2-OGT, protein O-GlcNAc levels and HCF-1 cleavage remained high after *Ogt* knockout, and accumulation of the necrosis-associated PARP-1 fragment was minimal. Cells expressing untagged ectopic *OGT*, which could not be selected for sufficient protein expression, had high amounts of the necrosis-associated PARP-1 fragment by day 3 (*SI Appendix*, Fig. S1*F*), consistent with OGT levels being insufficient to rescue growth in some cells (*SI Appendix*, Fig. S1 *E* and *F*). Taken together, our results show that OGT's canonical 1,036-amino acid isoform, when produced at sufficient levels, complements both cell growth and OGT's catalytic activities. Therefore, this single isoform encodes all of OGT's essential functions. A key advantage to ectopic expression of an *OGT* cDNA from a constitutive promoter is that O-GlcNAc-responsive mRNA regulation is bypassed, facilitating comparison of different OGT variants to identify those that support survival (44, 47–49).

Ser/Thr Glycosylation Is OGT's Only Essential Catalytic Activity. We tested a set of previously characterized OGT variants in our complementation system to determine which catalytic activities were necessary for cell survival (Fig. 2) (24, 25, 50–54). Ser/Thr glycosyation and HCF-1 cleavage occur in the same active site, and both reactions use uridine diphosphate-linked GlcNAc (UDP-GlcNAc) as a substrate (24, 51, 52). Active site residue K842 enables GlcNAc transfer for both reactions, so mutating this residue renders OGT catalytically inactive (24, 52, 54). An

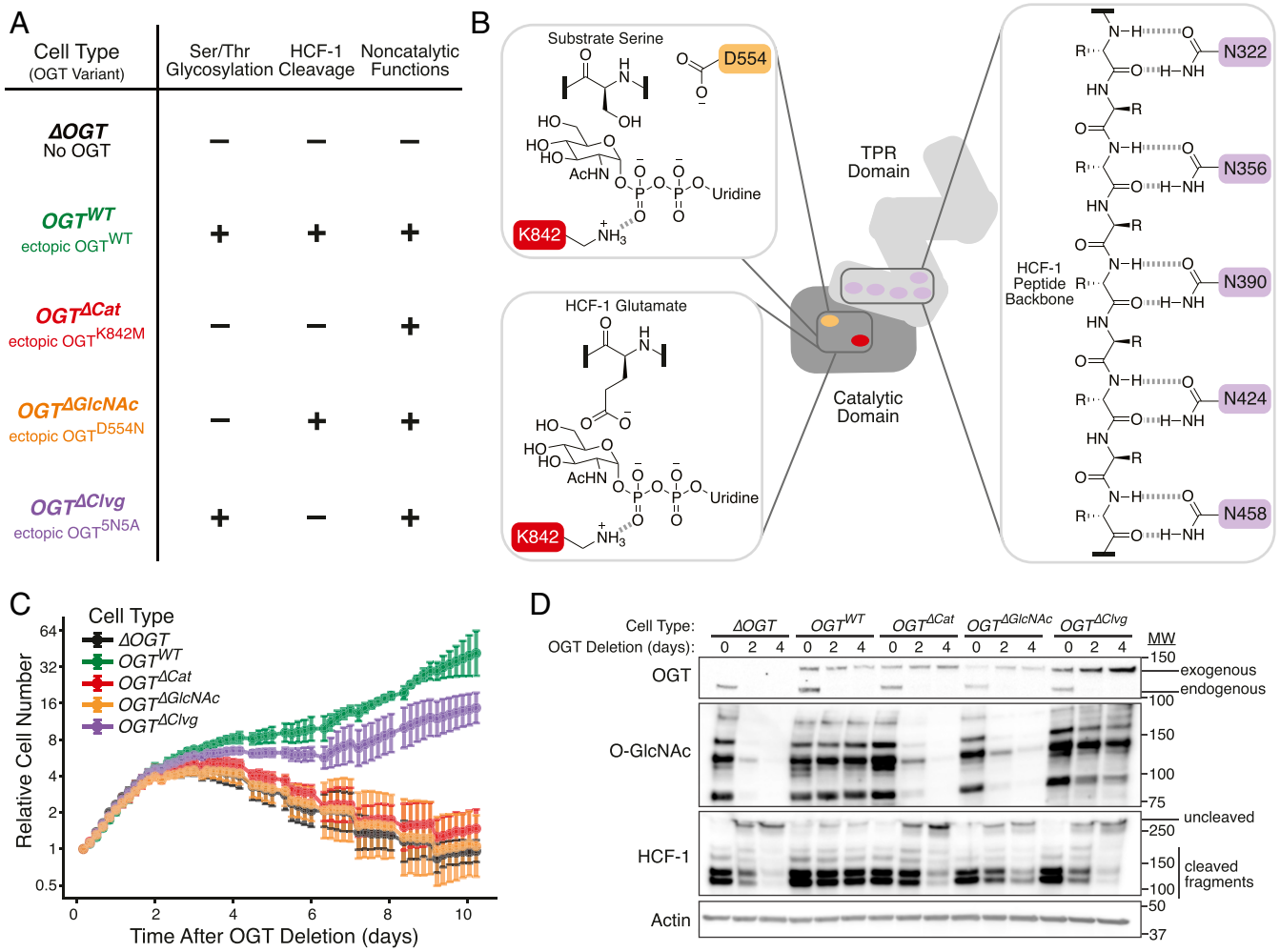

Fig. 2. OGT's only essential catalytic function is Ser/Thr glycosylation. (*A*) OGT variants with known in vitro activities can separate catalytic functions in living cells. Table shows cell type names and associated OGT variants. "–" indicates absence of OGT activity, while "+" indicates presence of OGT activity. "5N5A" refers to mutation of five conserved TPR Asn residues to Ala. (*B*) Mutation of key residues perturbs individual OGT activities. Active site residue K842 (red) is required for both Ser/Thr glycosylation (*Top Left*) and HCF-1 cleavage (*Bottom Left*). D554 (orange) mutation blocks Ser/Thr glycosylation but allows HCF-1 cleavage. Conserved TPR Asn residues (purple) bind substrates. Extensive binding is required for HCF-1 cleavage, but appreciable glycosylation is maintained upon mutation of five Asn residues to Ala (*SI Appendix*, Fig. S1*G*). R = side chains. (*C*) Cells without ability to add O-GlcNAc cease proliferation and die. Cells with *OGT* variants were imaged every 4 h after inducing *Ogt* knockout at t = 0. Relative cell number is based on normalized measurements of confluence from live cell imaging. Error bars are SD (n = 6 per condition). (*D*) Immunoblot analysis confirms the expected loss of either one or both catalytic activities depending on the ectopically produced OGT variant. See also *SI Appendix*, Fig. S1*G*.

OGT^{K842M} variant was used to assess whether OGT has noncatalytic functions that are sufficient for cell viability. Ser/Thr glycosylation requires residue D554 as a base to shuttle protons during the reaction, but this residue is not needed for HCF-1 proteolysis, which begins with glycosylation on a deprotonated glutamate side chain (*SI Appendix*, Fig. S1*B*) (24, 25, 50, 52). Mutating this residue therefore renders OGT inactive only for Ser/Thr glycosylation. An OGT^{D554N} variant was therefore used to test whether cell survival requires Ser/Thr glycosylation. During HCF-1 cleavage, the proteolytic repeat engages a network of five conserved asparagine residues in OGT's tetratricopeptide repeat (TPR) domain (24). Replacing these residues with Ala (OGT^{5N5A}) completely blocks HCF-1 cleavage (24). Ser/Thr glycosylation is attenuated with the OGT^{5N5A} mutant (53) but is not abolished (*SI Appendix*, Fig. S1*G*). Therefore, even though OGT^{5N5A} is an imperfect separation-of-function variant, we thought it might allow us to determine if HCF-1 cleavage is necessary for cell survival. Below we refer to cell lines completely lacking OGT as *ΔOGT*, to those producing OGT^{K842M} as $OGT^{\Delta Cat}$ for their lack of OGT catalytic activity, to those producing OGT^{D554N} as $OGT^{\Delta GlcNAc}$ for their lack of Ser/Thr glycosylation activity, and to those producing OGT^{5N5A} as $OGT^{\Delta Clvg}$ for their lack of HCF-1 cleavage activity (Fig. 2*A*).

We tested whether each OGT variant could complement loss of endogenous *Ogt*. Live cell microscopy showed that, like *ΔOGT* cells, $OGT^{\Delta Cat}$ or $OGT^{\Delta GlcNAc}$ cells grew for 2 d, then underwent growth arrest and eventually died (Fig. 2*C*). In contrast, OGT^{WT} and $OGT^{\Delta Clvg}$ cells continued to proliferate. Immunoblot analysis showed that only OGT^{WT} and $OGT^{\Delta Clvg}$ cells maintained protein O-GlcNAc levels (Fig. 2*D*). The levels of ectopically produced OGT increased over time in $OGT^{\Delta Clvg}$ cells until they were noticeably higher than in other cell lines lacking endogenous *Ogt*. We concluded that individual $OGT^{\Delta Clvg}$ clones with the highest ectopic OGT levels outgrew $OGT^{\Delta Clvg}$ cells with lower expression because higher OGT levels compensated for OGT^{5N5A}'s attenuated Ser/Thr glycosylation activity. Even with this increased OGT production, HCF-1 cleavage was blocked in the $OGT^{\Delta Clvg}$ cells (Fig. 2*D*). The survival of these cells showed that HCF-1 cleavage is not required for cell viability. Because all cells that retained Ser/Thr glycosylation activity survived, whereas all cells without this activity died, Ser/Thr glycosylation is OGT's only essential catalytic activity.

Chemically Induced Degradation Rapidly Separates OGT Functions. To study the direct cellular roles of the OGT variants, we sought to improve the speed of OGT depletion. Although genetic *Ogt* knockout is rapid, depletion of the endogenous OGT protein takes more than 2 d. By this time, cells completely lacking protein O-GlcNAc have undergone growth arrest and are in the process of dying. Additionally, Cre recombinase induces DNA damage signaling unrelated to OGT activity (*SI Appendix*, Fig. S1*F*) (55). We were concerned that the cell death process and DNA damage signaling would obscure direct cellular roles of OGT's catalytic activities. We speculated that if we could rapidly deplete wild-type OGT in the presence of a variant that retained only some activities, we might be able to deconvolute initial responses due to loss of an activity from other effects. Moreover, a rapid depletion system to synchronously alter cells' OGT activities might allow study of OGT variants that do not contain the full repertoire of functions required for viability.

To deplete wild-type OGT rapidly, we introduced an $FKBP12^{F36V}$-OGT fusion into inducible *Ogt* knockout MEFs (*SI Appendix*, Fig. S2*A*) to enable chemically induced protein degradation (56). $FKBP12^{F36V}$ provides a binding site for one-half of the heterobifunctional degrader molecule dTAG-13 (56). The other half of dTAG-13 recruits the E3 ligase cereblon, leading to ubiquitination and proteasomal degradation of $FKBP12^{F36V}$-OGT upon compound treatment (Fig. 3*A*). After knocking out endogenous *Ogt*, we isolated multiple MEF clones expressing only $FKBP12^{F36V}$-*OGT* (Fig. 3*B*). These clones were viable several weeks after endogenous *Ogt* removal, demonstrating that the $FKPB12^{F36V}$ tag did not interfere with essential OGT functions. Treatment of $FKBP12^{F36V}$-*OGT* cells with dTAG-13 depleted OGT within 1 h; depletion was sustained for 24 h (Fig. 3 *C*, *Inset*). We observed dose-dependent growth inhibition with maximal inhibition by 500 nM dTAG-13 (Fig. 3*C*), a concentration used for selective degradation of tagged proteins in several prior studies (56–58). Growth inhibition implied that OGT levels were sufficiently reduced to block OGT's growth-promoting cellular functions, providing a background in which we could assess how OGT's individual activities control cell physiology.

We next introduced separation-of-function OGT variants into clonal $FKBP12^{F36V}$-OGT cell lines (Fig. 3*D*). All cells had wild-type OGT activities before treatment, but at 24 and 48 h after dTAG-13 treatment, we only detected the OGT activities expected for each variant (Fig. 3*E*). Consistent with the OGT^{5N5A} mutant being partially impaired in Ser/Thr glycosylation, protein O-GlcNAc levels were moderately reduced in the $OGT^{\Delta Clvg}$ cells after dTAG-13 treatment.

We used quantitative proteomics in the different cell lines to query how cell physiology changed when specified OGT activities were removed (Fig. 3*F* and *SI Appendix*, Fig. S2*B*). Two biological replicates of each of our five $FKBP12^{F36V}$-OGT cell types (*ΔOGT*, OGT^{WT}, $OGT^{\Delta Cat}$, $OGT^{\Delta GlcNAc}$, and $OGT^{\Delta Clvg}$) were treated with dTAG-13 for 1 and 2 d; an untreated control (day 0) was also collected, and samples were labeled with isobaric tags to enable relative quantitation (59–61). Liquid chromatography/mass spectrometry (LC/MS) quantified 7,220 distinct proteins in all samples at all three time points (Dataset S1 and *SI Appendix*, Fig. S2*B*). For all cell lines, dTAG-13 treatment altered levels of more proteins at day 2 than day 1 (as measured by proteins changing >1.5-fold with P value of <0.01 in a two-sample t test, Fig. 3*G* and Dataset S2). At day 2, the fewest changes in protein levels were observed for OGT^{WT} and $OGT^{\Delta Clvg}$ cells (37 and 25 proteins, respectively) and the most were observed for *ΔOGT* cells (100 proteins). Cells expressing an OGT variant incapable of Ser/Thr glycosylation ($OGT^{\Delta GlcNAc}$ and $OGT^{\Delta Cat}$) had an intermediate number of altered proteins (65, 71). These results showed that Ser/Thr glycosylation plays a larger role in regulating protein levels than HCF-1 cleavage. Because there were more changes in *ΔOGT* than in the $OGT^{\Delta Cat}$ cells, the results also suggested that OGT may have physiologically important noncatalytic functions.

Simultaneous Comparison of Multiple Cell Lines Quantifies Effects of Individual OGT Activities. To identify proteins affected by individual OGT activities, we needed an analytical method to link changes in protein levels to the activities driving the changes. We reasoned that if a protein's abundance depended only on a single OGT activity, then the levels of that protein in a given cell line should differ based on whether that cell line retained the activity after dTAG-13 treatment (Fig. 4*A*). For example, levels of proteins controlled by Ser/Thr glycosylation or HCF-1 cleavage should differ between the two cell lines that retained that particular catalytic activity and the three cell lines without it. If a protein's abundance primarily depended on a noncatalytic function of OGT, levels should be similar for the four cell lines producing a copy of OGT but different in *ΔOGT* cells. Here, we name the $\log_2$ fold change in abundance of a protein upon losing an activity as the "effect size" of that OGT activity for that protein. Increased abundance of a protein when Ser/Thr glycosylation is blocked would lead to a positive Ser/Thr glycosylation effect size, whereas decreased abundance would produce a negative Ser/Thr glycosylation effect size. We hypothesized that

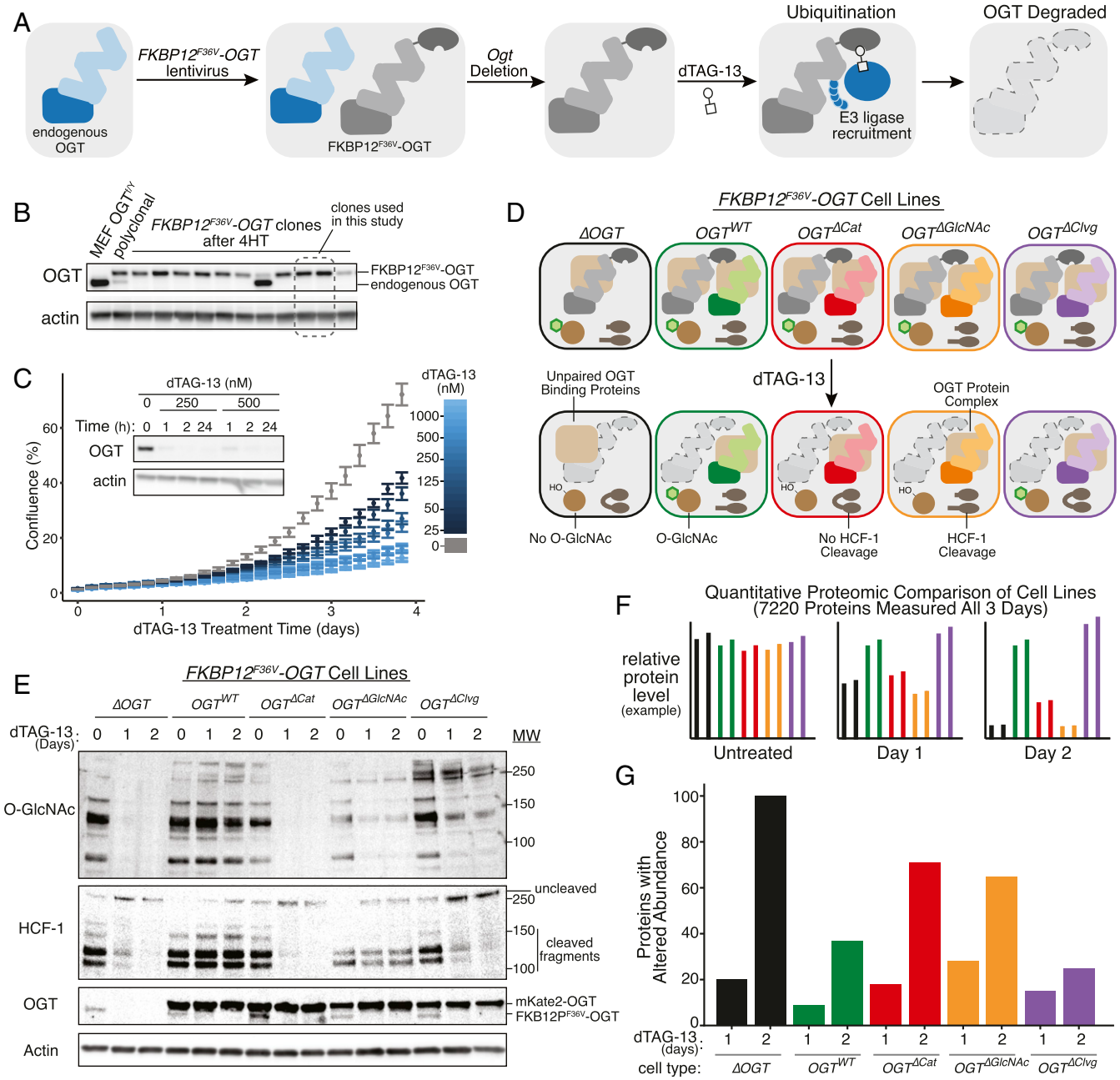

Fig. 3. Rapid OGT degradation reveals protein level changes due to loss of specified activities. (*A*) The dTAG system enables rapid, inducible OGT depletion. A copy of OGT tagged with FKBP12^{F36V} is used to replace endogenous OGT in MEFs. Treatment with heterobifunctional molecule dTAG-13 recruits endogenous E3 ligase cereblon to ubiquitinate FKBP12^{F36V}-OGT, leading to degradation. (*B*) Clonal MEFs containing FKBP12^{F36V}-OGT were isolated at 2 wk after *Ogt* knockout. Two clones lacking endogenous OGT were selected for further study. (*C*) FKBP12^{F36V}-OGT is rapidly degraded, leading to growth arrest. dTAG-13 treatment leads to dose-dependent growth arrest as measured by live cell imaging ($n = 6$, $n = 3$ per clone). Error bars are SEM. Submicromolar doses of dTAG-13 lead to rapid, durable degradation of FKBP12^{F36V}-OGT by immunoblot analysis (*Inset*). (*D*) Combining FKBP12^{F36V}-OGT with separation-of-function OGT variants allows synchronous separation of OGT activities. dTAG-13 treatment "unmasks" separation of function by rapidly removing wild-type OGT, allowing analysis of cells as specified OGT functions are lost. (*E*) Immunoblot analysis demonstrating separation of function within 1 d for *FKBP12^{F36V}-OGT* cells. mKate2-OGT bands show levels of OGT variants specifically added to each cell type. (*F*) Quantitative mass spectrometry profiles how altered OGT biochemistry changes protein levels proteome-wide. Isobaric peptide labeling and LC/MS^3-based protein quantitation enabled measurement of 7,220 proteins' levels across samples treated with dTAG-13 for 0, 1, or 2 d. Graphs represent hypothetical data. (*G*) More proteins changed levels with loss of OGT protein than with loss of its catalytic functions. Graph shows number of hits for each cell type after 1- or 2-d dTAG-13 treatment relative to untreated control (hits: >1.5-fold change in level and a *P* value <0.01 in a *t* test). See also *SI Appendix*, Fig. S2.

we could determine which proteins depended on which OGT activities by modeling protein levels as a linear combination of activity-specific effect sizes. Therefore, for each protein in the proteome, we used linear regression to calculate β_{GlcNAc}, β_{Clvg}, and β_{Ncat}, which are the activity-specific effect sizes that, when added together, describe how levels of that protein change when a specific set of OGT activities is removed (Fig. 4*B* and Dataset S3). By allowing us to use data from all five cell lines

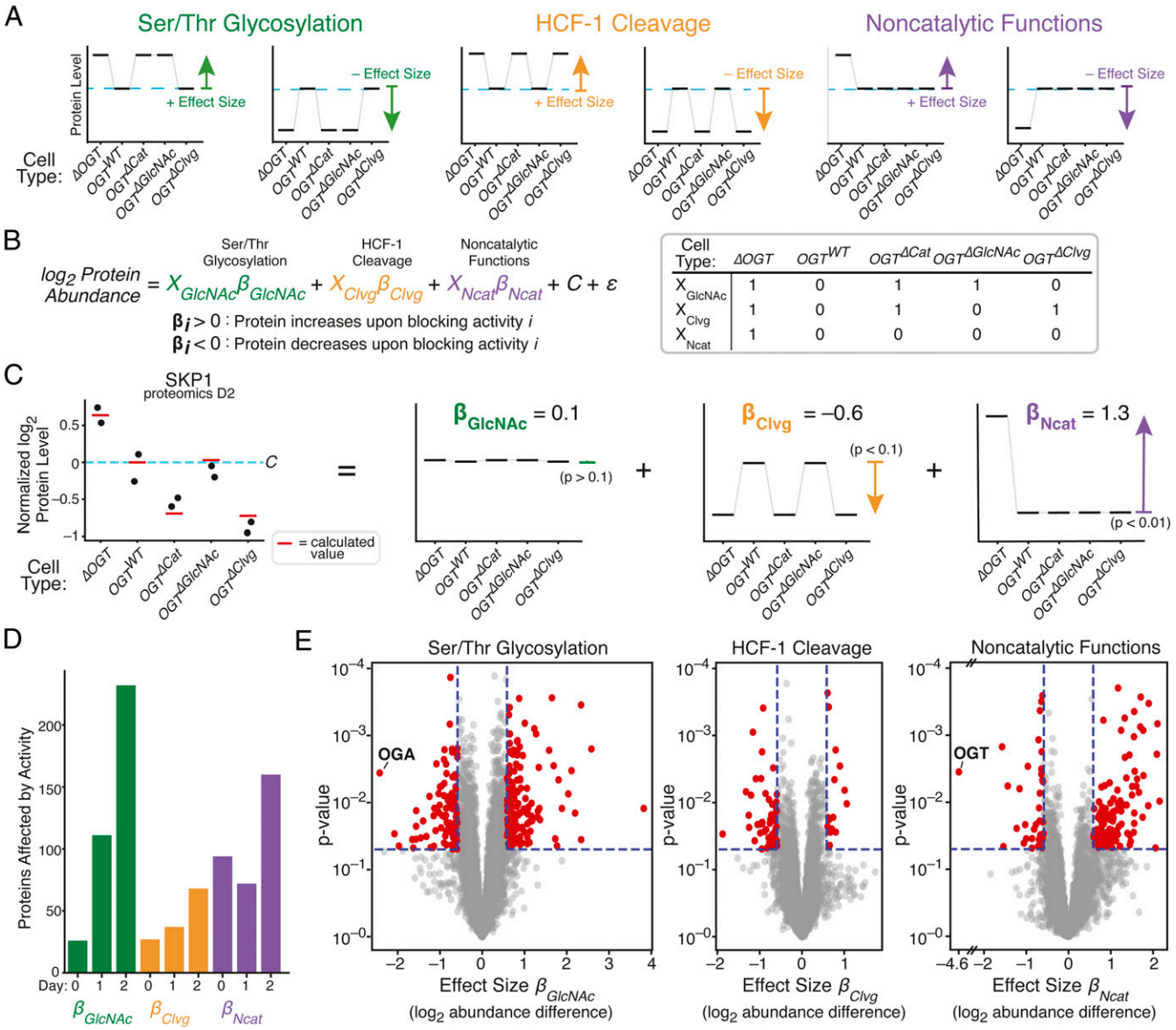

Fig. 4. Regression measures how single OGT activities alter levels of each protein. (*A*) Proteins whose levels are controlled by one OGT activity will show characteristic patterns among the five cell lines. Each graph represents a hypothetical protein controlled by a single activity; examples are shown for proteins that increase or decrease in response to inhibiting each activity. Protein level in OGT^{WT} cells is shown by blue dashed line. (*B*) Linear regression quantifies degree to which protein levels match the patterns corresponding to a given OGT activity. Effect sizes β_{GlcNAc}, β_{Clvg}, and β_{Ncat} are $\log_2$ fold change upon inhibiting an activity, and X_{GlcNAc}, X_{Clvg}, and X_{Ncat} indicate which cell lines lose a given OGT activity upon dTAG-13 treatment. C is average level in OGT^{WT} cells and ε is random variation unrelated to OGT activity. (*C*) Protein SKP1 is shown as a regression example; dots are measured abundance, red lines are calculated from linear regression, and individual effects are shown at *Right*. *P* values are shown for each effect. Level in OGT^{WT} cells is shown by blue dashed line. (*D*) Number of hits for each day for each OGT activity. (hits: $P < 0.05$ and effect size > $\log_2$ [1.5]). (*E*) Volcano plot showing β_{GlcNAc}, β_{Clvg}, and β_{Ncat} from 2 d of dTAG-13 treatment. OGT and OGA are highlighted as expected outliers. See also *SI Appendix*, Figs. S3 and S4.

simultaneously, this approach filtered out cell line-specific effects—for example, protein level changes due to reduced glycosylation in $OGT^{\Delta Clvg}$ cells—because these result in noisy effect sizes that do not meet *P* value cutoffs for statistical significance.

We observed that levels of some proteins depended on a single OGT activity, whereas others were best represented as a combination of OGT activities. For example, coactosin-like 1 (COTL1), an actin-binding protein, was less abundant in cells lacking HCF-1 cleavage activity (*SI Appendix*, Fig. S3 *A*, *Left*), while caldesmon 1 (CALD1), a protein involved in calcium-dependent actomyosin regulation, was more abundant in cells without a copy of OGT (*SI Appendix*, Fig. S3 *A*, *Middle*). The protein chaperone α-crystallin B (CRYAB), known to be O-GlcNAcylated and previously shown to be up-regulated in response to OGT knockout (40, 62), increased in cells lacking Ser/Thr glycosylation activity (*SI Appendix*, Fig. S3 *A*, *Right*). Therefore, we can attribute the increase in CRYAB abundance upon OGT knockout to loss of O-GlcNAc. In contrast to these proteins, which were dependent on a single OGT activity, SKP1, a protein in the SCF ubiquitin ligase complex, was sensitive to both loss of OGT, which led to increased abundance (β_{NCat} = 1.3), and to loss of HCF-1 cleavage, which led to decreased abundance ($\beta_{Clvg} = -0.6$), but not to loss of Ser/Thr glycosylation (Fig. 4*C*). By using this linear regression analysis, we could

therefore demonstrate that HCF-1 cleavage and noncatalytic OGT functions both regulate SKP1 levels, with a larger role for noncatalytic functions.

Several pieces of data showed that effect sizes generated across all three time points (*SI Appendix*, Fig. S3 *B* and *C* and Dataset S4) accurately reflected how levels of each protein responded to loss of individual OGT activities. Proteome-wide correlation analysis demonstrated that effect sizes for loss of each OGT activity corresponded to differences in protein abundance between any two sets of samples that differed by that OGT activity, both between different cell lines (*SI Appendix*, Fig. S4*A* and Dataset S5) and between untreated and treated samples of the same cell line (*SI Appendix*, Fig. S4*B*). Expected outliers in the data further validated the regression analysis (Fig. 4*E*). OGA abundance is known to decrease with low protein O-GlcNAc levels (40, 44), and we found that OGA had the most negative β_{GlcNAc} value after 2 d of dTAG-13 treatment. Furthermore, OGT had a negative β_{Ncat} value that corresponded to a striking 24-fold reduction in protein abundance; this result was reassuring because noncatalytic function effect sizes are defined by the presence or absence of OGT. We concluded that the regression analysis was an appropriate method to identify the proteins most affected by individual OGT activities.

We made two observations about the numbers of affected proteins and their changes over time (Fig. 4*D*). First, on day 0, few proteins were affected by Ser/Thr glycosylation or HCF-1 cleavage. We inferred that the presence of catalytically active $FKBP12^{F36V}$-OGT obscures differences in catalytic activity from other variants. In contrast, a substantial number of proteins were affected by noncatalytic functions at day 0. Noncatalytic roles are likely to involve stoichiometric binding interactions, and a second copy of OGT at day 0 would provide more protein to fulfill these roles. Second, after dTAG-13 treatment, loss of HCF-1 cleavage affected levels of a relatively small number of proteins compared to loss of OGT's other activities, implying a narrower role for this activity in regulating cell physiology. Loss of Ser/Thr glycosylation and noncatalytic functions each altered levels of more than 150 proteins by day 2, demonstrating a much larger impact of these activities.

Noncatalytic Functions and Ser/Thr Glycosylation Control Levels of Different Proteins. Proteome-wide analysis of effect sizes indicated that each OGT activity altered the levels of different sets of proteins (*SI Appendix*, Fig. S5*A*) and revealed that the majority of hit proteins had large effect sizes for only one OGT activity (Fig. 5*A*). Supporting the idea that different proteins are affected by different OGT activities, previously identified O-GlcNAc proteins were enriched among proteins with significant effect sizes for Ser/Thr glycosylation, and OGT interactors were enriched among proteins with significant effect sizes for noncatalytic functions (*SI Appendix*, Table S1) (33, 63). To examine the processes altered by individual OGT activities, we performed gene set enrichment analysis (GSEA) based on the effect sizes and their degree of statistical significance (Fig. 5*B*, *SI Appendix*, Fig. S5 *D* and *E* and Dataset S7) (64–66) to identify pathways affected by the different activities. Each OGT activity primarily affected different pathways from the others, although several pathways were affected by multiple OGT activities.

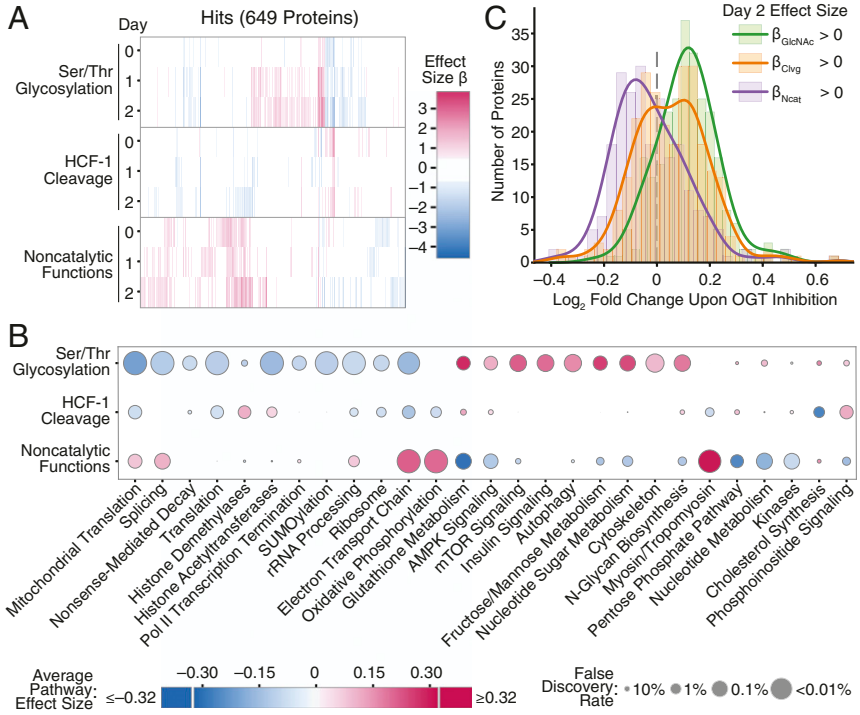

Fig. 5. Ser/Thr glycosylation and noncatalytic functions control distinct cellular processes. (*A*) Heatmap of effect sizes for all 649 protein hits for any OGT activity at any length of dTAG-13 treatment. OGT activity and length of dTAG-13 treatment shown on the *y* axis. Each *x* position is a distinct protein. (*B*) OGT activities control different pathways. Average effect sizes of all proteins (up to 25% change, effect size 0.32) in a given pathway are based on each OGT activity after 2 d of dTAG-13 treatment. Size of points corresponds to false discovery rate from GSEA. (*C*) Comparison of OGT inhibition and changes due to individual OGT activities. Histograms show $\log_2$ fold change in protein abundance upon OGT inhibition (67) for the set of proteins with positive day 2 β_{GlcNAc} (n = 263), β_{Clvg} (n = 264), and β_{Ncat} (n = 235) values. Lines show smoothed distribution for each set of proteins (Gaussian kernel bandwidth = 0.05). Only proteins significant in regression analysis (P < 0.01 for any effect size, 513 proteins) were analyzed. Proteins with positive effect sizes upon blocking any individual OGT activity had significantly more extreme changes in abundance upon OGT inhibition than expected by chance based on a Wilcoxon rank sum test (P value β_{GlcNAc} $<10^{-26}$, β_{Clvg} <0.01, β_{Ncat} $<10^{-10}$). See also *SI Appendix*, Figs. S5 and S6.

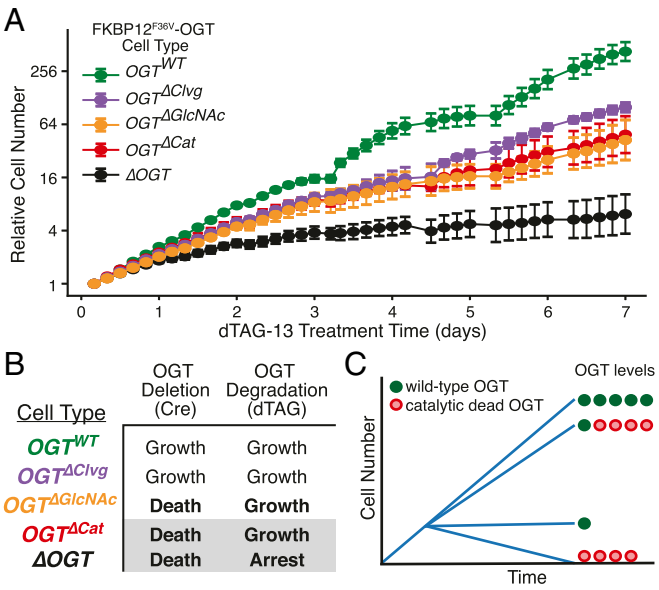

Fig. 6. OGT's noncatalytic roles are required for cell proliferation. (*A*) Cell growth over time of all FKBP12^{F36V}-OGT cell lines, as measured by live cell imaging. dTAG-13 treatment began at t = 0. Relative cell number is based on normalized measurements of confluence from live cell imaging. Error bars are SD (n = 6 per condition). (*B*) Growth outcomes for the Cre-based OGT deletion (Fig. 2) and dTAG-based OGT degradation systems (A). The degron-tagged Δ*OGT* cell line is viable because a very small amount of OGT remains after dTAG-13 treatment. (*C*) Schematic illustrating that OGT integrates catalytic and noncatalytic functions to promote cell growth.

Notably, OGT's noncatalytic function(s) were associated with oxidative phosphorylation and actin cytoskeleton components (Fig. 5*B* and *SI Appendix*, Fig. S5 *D* and *E*), while OGT's catalytic activities were associated with other areas of metabolism and numerous aspects of gene expression. Overall, the analysis showed that OGT's different biochemical activities—Ser/Thr glycosylation, HCF-1 cleavage, and noncatalytic functions—control different aspects of cell physiology.

We also compared the effects of altering individual OGT activities to the effects of inhibiting OGT with a small molecule. Using a previously reported dataset for OGT inhibition, we compared the changes in protein abundance observed after treating human HEK 293T cells with an OGT active site inhibitor to the effect sizes obtained from our genetic perturbations in MEFs (*SI Appendix*, Fig. S6 and Dataset S6) (67). Overall, we found that protein levels in 293T cells changed with OGT inhibition in the same direction as their mouse orthologs did when OGT's catalytic activities were removed (Fig. 5*C* and *SI Appendix*, Fig. S5*B*). The correspondence between protein abundance changes upon OGT active site inhibition and effect sizes for loss of OGT's catalytic activities provided independent evidence that these effect sizes are useful metrics for quantifying the contributions of OGT's catalytic activities to regulating protein abundance. Moreover, because inhibiting OGT in HEK 293T cells and removing OGT's catalytic activities in MEFs affected similar biological pathways (*SI Appendix*, Fig. S5 *C* and *D* and Dataset S7), we have inferred that OGT's catalytic activities play consistent roles in controlling cell physiology in different mammals.

Unexpectedly, we also observed a relationship between OGT inhibition and OGT's noncatalytic functions. Inhibition altered protein levels in the opposite direction from removing OGT's noncatalytic functions, a phenomenon observed at both the protein and biological pathway levels (Fig. 5*C* and *SI Appendix*, Fig. S5 *B–D*). It is well known that OGT levels rapidly increase upon loss of protein O-GlcNAcylation (44, 48, 67, 68), with the rapid increases driven by splicing and transcriptional controls that we removed in the MEF system. These mechanisms were thought to serve as a means to restore normal O-GlcNAc levels. However, we interpret the inverse correlation between protein-level changes after small molecule OGT inhibition and effect sizes for removing OGT's noncatalytic functions as evidence that increased OGT abundance is important independent of altering OGT catalytic activity. Therefore, OGT's noncatalytic functions contribute to the normal cellular response to reduced O-GlcNAcylation.

Noncatalytic Functions Are Required for Cell Proliferation. Given that our analysis strongly implicated OGT noncatalytic functions in controlling cell physiology, we wondered if these functions were important for cell growth. To test if OGT's noncatalytic activities contribute to cell proliferation, we tracked growth of our five FKBP12^{F36V}-OGT cell lines in the presence of enough dTAG-13 to suppress proliferation of *ΔOGT* cells (Fig. 6*A*). As expected, the OGT^{WT} and $OGT^{\Delta Clvg}$ cells, which can carry out Ser/Thr glycosylation, grew in the presence of the degrader compound; however, the $OGT^{\Delta GlcNAc}$ and $OGT^{\Delta Cat}$ cells, which are nonviable in the Cre-based deletion system, also grew (Fig. 6 *A* and *B*). Because the amounts of catalytically active FKBP12^{F36V}-OGT remaining after dTAG-13 treatment are too low to permit cell proliferation, growth of the $OGT^{\Delta Cat}$ cells requires noncatalytic roles of OGT (Fig. 6*C*).

Discussion

This study identified the OGT functions that are essential for growth of mammalian cells. First, by replacing OGT with variants impaired in selected activities, we determined that protein O-GlcNAcylation is required for cell survival. HCF-1 cleavage is not. Next, by using inducible protein degradation and a broadly applicable proteomic analysis method to deconvolute the roles of variants that are deficient in one or more OGT activities, we demonstrated that OGT has noncatalytic roles that regulate protein levels independent of catalysis. We also showed that these noncatalytic functions are sufficient to drive growth when there is insufficient wild-type OGT to support cell proliferation. Taken together, our results show that OGT has two essential functions, Ser/Thr glycosylation and a noncatalytic role.

OGT's catalytic and noncatalytic functions evidently cooperate to control cell proliferation. If no OGT is present, or if OGT is present but cannot catalyze any Ser/Thr glycosylation, cells die. If wild-type OGT is present, but at extremely low levels, cells are viable but remain in a growth-arrested state. Adding back catalytically inactive OGT rescues cell proliferation even though protein O-GlcNAc levels remain low. Therefore, providing sufficient OGT to fulfill its stoichiometric noncatalytic roles promotes cell proliferation even if only a small amount of O-GlcNAc is present. It remains to be established how OGT's noncatalytic functions promote cell proliferation, but possibilities include binding other proteins to stabilize them, to alter their localization, or to scaffold the formation of larger complexes.

The importance of OGT's noncatalytic functions for cell growth helps explain a previously observed discrepancy between genetic OGT knockout and OGT inhibition. Cells die upon knockout (40) but not when OGT is inhibited. Death occurs in the former case because both O-GlcNAc signaling and OGT's noncatalytic functions are removed. With inhibition, low levels of Ser/Thr glycosylation persist. The reduced protein O-GlcNAc levels trigger a rapid increase in OGT abundance through altered splicing and transcription (44, 48, 67). When the increase in OGT abundance is sufficient to overcome inhibition, O-GlcNAc levels recover. Whether or not they recover, signaling through OGT's noncatalytic functions increases because there is

more OGT protein available. Noncatalytic functions drive cell proliferation even when O-GlcNAc levels remain very low.

OGT's noncatalytic functions may be important for OGT's role as a nutrient sensor. Low nutrients lead to reduced cytosolic UDP-GlcNAc levels (8, 22), leading to a transient reduction in O-GlcNAc levels that is followed by rapid up-regulation of OGT (68). If protein O-GlcNAc levels remain low even though OGT abundance is high, noncatalytic signaling may become especially important. We suggest that OGT uses both its catalytic and noncatalytic functions to respond to environmental changes, which may allow for varied responses to different cellular cues.

By quantifying how much each OGT activity impacts cellular protein abundance, we have identified the biological pathways most affected by each OGT activity. Consistent with known roles for O-GlcNAc, we found that Ser/Thr glycosylation broadly regulates metabolism and gene expression, with enriched pathways, including splicing (44), translation (69–71), and autophagy (72–74). Among the pathways linked to OGT's noncatalytic activities are oxidative phosphorylation, the electron transport chain, and components of the actin cytoskeleton, consistent with prior data suggesting OGT binds to the actin-regulating E-cadherin/beta-catenin complex (39). We also note that a previous report showed that proteins involved in oxidative phosphorylation and electron transport were down-regulated upon OGT overexpression (75), consistent with our finding that blocking OGT's noncatalytic functions leads to an increase in the levels of these proteins. These previous studies attributed altered abundance of proteins involved in respiration to increased O-GlcNAc, but our results suggest that OGT's noncatalytic functions also contribute substantially to altering levels of these proteins.

Our data show that OGT's glycosyltransferase and noncatalytic OGT functions can cooperate within the same cellular pathway to alter cell physiology. When nutrients are low or OGT is inhibited, signaling through Ser/Thr glycosylation is reduced, but elevated OGT levels lead to increased signaling through OGT's noncatalytic functions. Our effect sizes measure the response of protein levels to loss of an OGT activity so an increase in noncatalytic signaling would lead to protein-level changes in the opposite direction from the noncatalytic effect sizes. As a result, upon nutrient deprivation, Ser/Thr glycosylation and noncatalytic functions cooperate to change levels in the same direction for proteins with oppositely signed effect sizes. Our analytical method identifies pathways dominated by one activity as well as pathways where both catalytic and noncatalytic OGT functions substantially contribute to regulation (Fig. 5). Going forward, it will be critical to determine whether effects of genetic knockdown are due to loss of O-GlcNAc, loss of OGT's noncatalytic functions, or both.

HCF-1 cleavage affected a more limited number of cellular processes than OGT's other activities, but it remains a central player in OGT biology. We found that the cleavage activity affects histone modification pathways, which include known interactors of HCF-1 (76, 77), as well as lipid metabolism and peroxisome-related processes (Fig. 5*C*, *SI Appendix*, Fig. S5*D*, and Dataset S7), which have been linked to HCF-1 based on hepatocyte-specific HCF-1 knockout mice (78). Because HCF-1 is one of OGT's most common cellular binding partners (26, 29, 32, 33, 77) and is O-GlcNAcylated in addition to being proteolyzed, it integrates all three of OGT's biochemical activities. HCF-1 regulates transcription through participation in several chromatin-modifying complexes (33, 77, 79), and recent evidence suggests it is directly involved in altering gene expression in response to nutrient cues, including cues that result in altered O-GlcNAc (32, 33, 80). Moreover, both O-GlcNAc modification and cleavage of HCF-1 have been shown to change its binding partners and consequently alter downstream gene expression (32, 81). Effects of HCF-1 cleavage were previously investigated by altering HCF-1 structure. The ability to disrupt cleavage by varying OGT rather than by altering HCF-1 may have advantages for understanding the role of HCF-1 in gene expression and the interplay of cleavage with HCF-1 O-GlcNAcylation and OGT binding.

We expect the genetic systems and approaches described here will be useful for addressing long-standing questions about OGT. One important question is how O-GlcNAcylation supports cell viability. It is possible that a small number of OGT substrates require O-GlcNAc modification to carry out essential functions. If so, these might be found by identifying the proteins that are still modified by OGT variants that have lost the ability to glycosylate most substrates. Similarly, the ability to introduce OGT variants into cells and either delete or deplete wild-type OGT will help elucidate the binding partners through which OGT engages in noncatalytic signaling. These binding partners likely include other proteins, but may also include nucleic acids or other molecules. OGT's TPR domain has been implicated in binding interactions (3, 34), and the ability to modify this domain to disrupt binding should be helpful in dissecting OGT function. The approaches and analytical strategy we have developed to quantify effects of OGT's activities on protein levels can also be adapted to understand other multifunctional proteins. Moreover, although we used protein abundance to quantify effect sizes in the studies here, other quantitative phenotypes such as transcriptomic measurements can also be used to link particular functions to pathways (82). Last, by extending these approaches to alternative cell types, we anticipate that we may be able to determine which effects of OGT's activities are general and which are only relevant in the signaling context of a particular cell type.

Finally, we note that the results here have implications relevant to OGT-targeting therapeutics. OGT has been identified as a potential target in multiple diseases, including cancer (14–17, 47, 49) and metabolic disease (8, 18–21). Many of the studies implicating OGT in these diseases used genetic perturbations that blocked catalytic and noncatalytic signaling simultaneously. However, OGT deletion and depletion phenotypes are different from phenotypes due to OGT active site inhibition. Antiproliferative effects are more likely to occur from removing OGT entirely than from blocking its active site because, as we have shown, cells can proliferate with very low catalytic activity if there is sufficient OGT protein to fulfill noncatalytic roles. Therefore, targeting OGT for cancer therapy may require either a targeted protein degradation approach (83) that disrupts both catalytic and noncatalytic OGT activities or a strategy that exploits synthetic lethality between OGT inhibition and targeting another pathway (84). By contrast, if metabolic syndrome indeed results from excess Ser/Thr glycosylation, it may be possible to use OGT inhibitors chronically to reduce protein O-GlcNAc levels; however, inhibitor treatment may lead to chronic elevation of OGT levels, and our findings show that a persistent increase in OGT may affect cell physiology independent of catalysis.

Materials and Methods

Plasmids and Cloning. Plasmids for protein expression and lentivirus production were generated as described in *SI Appendix*. Mutations were introduced by Q5 mutagenesis or Gibson assembly.

Cells and Lentivirus. The MEF cell line was maintained as previously described (40). Lentivirus was produced in HEK 293T cells and infections of MEF cells were carried out as described in *SI Appendix*. Knockout of OGT was performed as previously described (40). Degradation of $FKBP12^{F36V}$-OGT was carried out by changing to media containing 500 nM dTAG-13. Cell lysis and immunoblot analysis were carried out as described in *SI Appendix*.

Growth Assays. All growth assays were carried out in 96-well plates using the Essen Incucyte Zoom platform as described in *SI Appendix*. Relative cell

number was based upon confluence normalized to initial confluence. To enable long-term tracking of growth, cells that reached 85% confluence were split 1:3 and replated for continued growth, with relative cell number reflecting continued growth from point of splitting.

Quantitative Proteomics. Samples were prepared, labeled with isobaric tandem mass tag (TMT) labels, fractionated by high performance liquid chromatography (HPLC), and analyzed by LC/MS^3 as previously described (59–61), with further details in *SI Appendix*. A normalization sample of peptides from all other samples was generated by mixing all 30 samples in the same tube before TMT labeling. LC/MS data were analyzed as described in *SI Appendix* to yield relative protein abundance. For analysis across days, each protein's abundance was divided by protein abundance in the normalization sample for that day.

Linear Regression Analysis. Linear regression as described in Fig. 4*B* was used to analyze each protein. Samples were randomly shuffled 10^6 times to generate background distributions to determine *P* values for each regression coefficient (effect size). For linear regression across multiple days, 10 coefficients (3 d of three effect sizes plus a constant representing baseline abundance) were included with 30 samples, with the same procedure used to generate *P* values. Further details are available in *SI Appendix*.

Pathway Analysis. GSEA was carried out using either effect size or $\log_{10}$ of *P* value (negative $\log_{10}$ if effect size was positive). Pathways were considered significant if they met a 10% false discovery rate (FDR) cutoff in both analyses and a 1% cutoff in either analysis. Further details are provided in *SI Appendix*.

Comparison to OGT Inhibitor. Data from Martin et al. (67) as presented in the supplemental information of that publication were aligned on the basis of gene orthology and analyzed as described in the text. Further details of analysis are available in *SI Appendix*.

Data Availability. Request for materials should be directed to suzanne_walker@hms.harvard.edu. All plasmids generated in this study are available through Addgene (*SI Appendix*, Table S3). Raw proteomics data have been deposited to the ProteomeXchange (85) via PRIDE (86) with identifier PXD022654. Code for analysis is available on Github (https://github.com/SuzanneWalkerLab/NoncatalyticOGT/). All study data are included in the article and supporting information.

ACKNOWLEDGMENTS. We thank Prof. Connie Cepko for lentivirus advice and the Immunology Flow Cytometry Core Facility at Harvard Medical School for cell sorting. We thank Prof. Steven P. Gygi for providing access to facilities for mass spectrometry. This work was supported by the NIH (GM094263 to S.W.; GM132129 to J.A.P.; K12HL141952 and CA230978 to N.E.Z.; and T32 GM095450 to Z.G.L., S.C.P, and G.Q.F.) and the Katherine L. and Steven C. Pinard Research Fund (N.S.G.), with additional support in the form of pre- and postdoctoral fellowships (NSF grant DGE1745303 to S.C.P.; F32 GM129889 to C.M.J.; 5F31GM116451 to M.S.; and American Cancer Society Postdoctoral Fellowship PF-17-010-01-CDD to B.N.). Aid and equipment for live cell imaging were provided by Dr. Clarence Yapp and the Laboratory for Systems Pharmacology at Harvard Medical School, which is supported in part by NIH grants P50GM107618 and U54CA225088, Defense Advanced Research Projects Administration grant W911NF-19-2-0017, and the Ludwig Center at Harvard Medical School.

1. M. Jöud, M. Möller, M. L. Olsson, Identification of human glycosyltransferase genes expressed in erythroid cells predicts potential carbohydrate blood group loci. *Sci. Rep.* **8**, 6040 (2018).
2. K. J. Karczewski *et al.*; Genome Aggregation Database Consortium, The mutational constraint spectrum quantified from variation in 141,456 humans. *Nature* **581**, 434–443 (2020).
3. Z. G. Levine, S. Walker, The biochemistry of O-GlcNAc transferase: Which functions make it essential in mammalian cells? *Annu. Rev. Biochem.* **85**, 631–657 (2016).
4. N. O'Donnell, N. E. Zachara, G. W. Hart, J. D. Marth, Ogt-dependent X-chromosome-linked protein glycosylation is a requisite modification in somatic cell function and embryo viability. *Mol. Cell. Biol.* **24**, 1680–1690 (2004).
5. R. Shafi *et al.*, The O-GlcNAc transferase gene resides on the X chromosome and is essential for embryonic stem cell viability and mouse ontogeny. *Proc. Natl. Acad. Sci. U.S.A.* **97**, 5735–5739 (2000).
6. N. Zachara, Y. Akimoto, G. W. Hart, "The O-GlcNAc modification" in *Essentials of Glycobiology*, A. Varki, *et al.*, Eds. (Cold Spring Harbor Laboratory Press, ed. 3, 2015).
7. R. Trapannone, D. Mariappa, A. T. Ferenbach, D. M. F. van Aalten, Nucleocytoplasmic human O-GlcNAc transferase is sufficient for O-GlcNAcylation of mitochondrial proteins. *Biochem. J.* **473**, 1693–1702 (2016).
8. X. Yang, K. Qian, Protein O-GlcNAcylation: Emerging mechanisms and functions. *Nat. Rev. Mol. Cell Biol.* **18**, 452–465 (2017).
9. D. L. Dong, G. W. Hart, Purification and characterization of an O-GlcNAc selective N-acetyl-beta-D-glucosaminidase from rat spleen cytosol. *J. Biol. Chem.* **269**, 19321–19330 (1994).
10. Y. Gao, L. Wells, F. I. Comer, G. J. Parker, G. W. Hart, Dynamic O-glycosylation of nuclear and cytosolic proteins: Cloning and characterization of a neutral, cytosolic beta-N-acetylglucosaminidase from human brain. *J. Biol. Chem.* **276**, 9838–9845 (2001).
11. I. Han, E. S. Oh, J. E. Kudlow, Responsiveness of the state of O-linked N-acetylglucosamine modification of nuclear pore protein p62 to the extracellular glucose concentration. *Biochem. J.* **350**, 109–114 (2000).
12. K. Liu, A. J. Paterson, E. Chin, J. E. Kudlow, Glucose stimulates protein modification by O-linked GlcNAc in pancreatic β cells: Linkage of O-linked GlcNAc to β cell death. *Proc. Natl. Acad. Sci. U.S.A.* **97**, 2820–2825 (2000).
13. N. E. Zachara *et al.*, Dynamic O-GlcNAc modification of nucleocytoplasmic proteins in response to stress. A survival response of mammalian cells. *J. Biol. Chem.* **279**, 30133–30142 (2004).
14. N. M. Akella *et al.*, O-GlcNAc transferase regulates cancer stem-like potential of breast cancer cells. *Mol. Cancer Res.* **18**, 585–598 (2020).
15. C. M. Ferrer *et al.*, O-GlcNAcylation regulates cancer metabolism and survival stress signaling via regulation of the HIF-1 pathway. *Mol. Cell* **54**, 820–831 (2014).
16. C. M. Ferrer, V. L. Sodi, M. J. Reginato, O-GlcNAcylation in cancer biology: Linking metabolism and signaling. *J. Mol. Biol.* **428**, 3282–3294 (2016).
17. H. M. Itkonen *et al.*, O-GlcNAc transferase integrates metabolic pathways to regulate the stability of c-MYC in human prostate cancer cells. *Cancer Res.* **73**, 5277–5287 (2013).
18. M.-D. Li *et al.*, Adipocyte OGT governs diet-induced hyperphagia and obesity. *Nat. Commun.* **9**, 5103 (2018).
19. H. Shi *et al.*, Skeletal muscle O-GlcNAc transferase is important for muscle energy homeostasis and whole-body insulin sensitivity. *Mol. Metab.* **11**, 160–177 (2018).
20. K. Vaidyanathan, L. Wells, Multiple tissue-specific roles for the O-GlcNAc post-translational modification in the induction of and complications arising from type II diabetes. *J. Biol. Chem.* **289**, 34466–34471 (2014).
21. Y. Yang *et al.*, O-GlcNAc transferase inhibits visceral fat lipolysis and promotes diet-induced obesity. *Nat. Commun.* **11**, 181 (2020).
22. M. R. Bond, J. A. Hanover, A little sugar goes a long way: The cell biology of O-GlcNAc. *J. Cell Biol.* **208**, 869–880 (2015).
23. G. W. Hart, C. Slawson, G. Ramirez-Correa, O. Lagerlof, Cross talk between O-GlcNAcylation and phosphorylation: Roles in signaling, transcription, and chronic disease. *Annu. Rev. Biochem.* **80**, 825–858 (2011).
24. M. B. Lazarus *et al.*, HCF-1 is cleaved in the active site of O-GlcNAc transferase. *Science* **342**, 1235–1239 (2013).
25. J. Janetzko, S. A. Trauger, M. B. Lazarus, S. Walker, How the glycosyltransferase OGT catalyzes amide bond cleavage. *Nat. Chem. Biol.* **12**, 899–901 (2016).
26. F. Capotosti *et al.*, O-GlcNAc transferase catalyzes site-specific proteolysis of HCF-1. *Cell* **144**, 376–388 (2011).
27. E. Julien, W. Herr, Proteolytic processing is necessary to separate and ensure proper cell growth and cytokinesis functions of HCF-1. *EMBO J.* **22**, 2360–2369 (2003).
28. E. Julien, W. Herr, A switch in mitotic histone H4 lysine 20 methylation status is linked to M phase defects upon loss of HCF-1. *Mol. Cell* **14**, 713–725 (2004).
29. S. Daou *et al.*, Crosstalk between O-GlcNAcylation and proteolytic cleavage regulates the host cell factor-1 maturation pathway. *Proc. Natl. Acad. Sci. U.S.A.* **108**, 2747–2752 (2011).
30. W. D. Cheung, G. W. Hart, AMP-activated protein kinase and p38 MAPK activate O-GlcNAcylation of neuronal proteins during glucose deprivation. *J. Biol. Chem.* **283**, 13009–13020 (2008).
31. W. D. Cheung, K. Sakabe, M. P. Housley, W. B. Dias, G. W. Hart, O-linked beta-N-acetylglucosaminyltransferase substrate specificity is regulated by myosin phosphatase targeting and other interacting proteins. *J. Biol. Chem.* **283**, 33935–33941 (2008).
32. E. A. Lane *et al.*, HCF-1 regulates de novo lipogenesis through a nutrient-sensitive complex with ChREBP. *Mol. Cell* **75**, 357–371.e7 (2019).
33. H.-B. Ruan *et al.*, O-GlcNAc transferase/host cell factor C1 complex regulates gluconeogenesis by modulating PGC-1α stability. *Cell Metab.* **16**, 226–237 (2012).
34. H. M. Stephen, J. L. Praissman, L. Wells, Generation of an unbiased interactome for the tetratricopeptide repeat domain of O-GlcNAc transferase indicates a role for the enzyme in intellectual disability. *bioRxiv*:2020.07.30.229930 (30 July 2020).
35. S. J. Urso, M. Comly, J. A. Hanover, T. Lamitina, The O-GlcNAc transferase OGT is a conserved and essential regulator of the cellular and organismal response to hypertonic stress. *PLoS Genet.* **16**, e1008821 (2020).
36. A. C. Giles *et al.*, A complex containing the *O*-GlcNAc transferase OGT-1 and the ubiquitin ligase EEL-1 regulates GABA neuron function. *J. Biol. Chem.* **294**, 6843–6856 (2019).
37. J. A. Hanover *et al.*, A Caenorhabditis elegans model of insulin resistance: Altered macronutrient storage and dauer formation in an OGT-1 knockout. *Proc. Natl. Acad. Sci. U.S.A.* **102**, 11266–11271 (2005).
38. D. Mariappa *et al.*, Dual functionality of O-GlcNAc transferase is required for Drosophila development. *Open Biol.* **5**, 150234 (2015).
39. H. Liu *et al.*, Inhibition of E-cadherin/catenin complex formation by O-linked N-acetylglucosamine transferase is partially independent of its catalytic activity. *Mol. Med. Rep.* **13**, 1851–1860 (2016).

40. Z. Kazemi, H. Chang, S. Haserodt, C. McKen, N. E. Zachara, O-linked β-N-acetylglucosamine (O-GlcNAc) regulates stress-induced heat shock protein expression in a GSK-3β-dependent manner. *J. Biol. Chem.* **285**, 39096–39107 (2010).
41. E. Campeau *et al*., A versatile viral system for expression and depletion of proteins in mammalian cells. *PLoS One* **4**, e6529 (2009).
42. D. Shcherbo *et al*., Far-red fluorescent tags for protein imaging in living tissues. *Biochem. J.* **418**, 567–574 (2009).
43. A. Ramezani, R. G. Hawley, Strategies to insulate lentiviral vector-expressed transgenes. *Methods Mol. Biol.* **614**, 77–100 (2010).
44. Z.-W. Tan, *et al*., O-GlcNAc regulates gene expression by controlling detained intron splicing. *Nucleic Acids Res.* **48**, 5656–5669 (2020).
45. G. V. Chaitanya, A. J. Steven, P. P. Babu, PARP-1 cleavage fragments: Signatures of cell-death proteases in neurodegeneration. *Cell Commun. Signal.* **8**, 31 (2010).
46. S. Gobeil, C. C. Boucher, D. Nadeau, G. G. Poirier, Characterization of the necrotic cleavage of poly(ADP-ribose) polymerase (PARP-1): Implication of lysosomal proteases. *Cell Death Differ.* **8**, 588–594 (2001).
47. Y. Liu *et al*., Suppression of OGT by microRNA24 reduces FOXA1 stability and prevents breast cancer cells invasion. *Biochem. Biophys. Res. Commun.* **487**, 755–762 (2017).
48. S.-K. Park *et al*., A conserved splicing silencer dynamically regulates O-GlcNAc transferase intron retention and O-GlcNAc homeostasis. *Cell Rep.* **20**, 1088–1099 (2017).
49. K. Qian *et al*., Transcriptional regulation of *O*-GlcNAc homeostasis is disrupted in pancreatic cancer. *J. Biol. Chem.* **293**, 13989–14000 (2018).
50. V. Kapuria *et al*., Proteolysis of HCF-1 by Ser/Thr glycosylation-incompetent O-GlcNAc transferase:UDP-GlcNAc complexes. *Genes Dev.* **30**, 960–972 (2016).
51. M. B. Lazarus, Y. Nam, J. Jiang, P. Sliz, S. Walker, Structure of human O-GlcNAc transferase and its complex with a peptide substrate. *Nature* **469**, 564–567 (2011).
52. M. B. Lazarus *et al*., Structural snapshots of the reaction coordinate for O-GlcNAc transferase. *Nat. Chem. Biol.* **8**, 966–968 (2012).
53. Z. G. Levine *et al*., O-GlcNAc transferase recognizes protein substrates using an asparagine ladder in the tetratricopeptide repeat (TPR) superhelix. *J. Am. Chem. Soc.* **140**, 3510–3513 (2018).
54. M. Schimpl *et al*., O-GlcNAc transferase invokes nucleotide sugar pyrophosphate participation in catalysis. *Nat. Chem. Biol.* **8**, 969–974 (2012).
55. A. Loonstra *et al*., Growth inhibition and DNA damage induced by Cre recombinase in mammalian cells. *Proc. Natl. Acad. Sci. U.S.A.* **98**, 9209–9214 (2001).
56. B. Nabet *et al*., The dTAG system for immediate and target-specific protein degradation. *Nat. Chem. Biol.* **14**, 431–441 (2018).
57. M. A. Erb *et al*., Transcription control by the ENL YEATS domain in acute leukaemia. *Nature* **543**, 270–274 (2017).
58. H.-T. Huang *et al*., MELK is not necessary for the proliferation of basal-like breast cancer cells. *eLife* **6**, e26693 (2017).
59. G. C. McAlister *et al*., Increasing the multiplexing capacity of TMTs using reporter ion isotopologues with isobaric masses. *Anal. Chem.* **84**, 7469–7478 (2012).
60. G. C. McAlister *et al*., MultiNotch MS3 enables accurate, sensitive, and multiplexed detection of differential expression across cancer cell line proteomes. *Anal. Chem.* **86**, 7150–7158 (2014).
61. J. Navarrete-Perea, Q. Yu, S. P. Gygi, J. A. Paulo, Streamlined tandem mass tag (SL-TMT) protocol: An efficient strategy for quantitative (Phospho)proteome profiling using tandem mass tag-synchronous precursor selection-MS3. *J. Proteome Res.* **17**, 2226–2236 (2018).
62. E. P. Roquemore *et al*., Vertebrate lens alpha-crystallins are modified by O-linked N-acetylglucosamine. *J. Biol. Chem.* **267**, 555–563 (1992).
63. C. M. Woo *et al*., Mapping and quantification of over 2000 O-linked glycopeptides in activated human T cells with isotope-targeted glycoproteomics (isotag). *Mol. Cell. Proteomics* **17**, 764–775 (2018).
64. B. Jassal *et al*., The reactome pathway knowledgebase. *Nucleic Acids Res.* **48**, D498–D503 (2020).
65. M. Kanehisa, S. Goto, KEGG: Kyoto encyclopedia of genes and genomes. *Nucleic Acids Res.* **28**, 27–30 (2000).
66. A. Subramanian *et al*., Gene set enrichment analysis: A knowledge-based approach for interpreting genome-wide expression profiles. *Proc. Natl. Acad. Sci. U.S.A.* **102**, 15545–15550 (2005).
67. S. E. S. Martin *et al*., Structure-based evolution of low nanomolar O-GlcNAc transferase inhibitors. *J. Am. Chem. Soc.* **140**, 13542–13545 (2018).
68. R. P. Taylor *et al*., Glucose deprivation stimulates O-GlcNAc modification of proteins through up-regulation of O-linked N-acetylglucosaminyltransferase. *J. Biol. Chem.* **283**, 6050–6057 (2008).
69. X. Li *et al*., O-GlcNAcylation of core components of the translation initiation machinery regulates protein synthesis. *Proc. Natl. Acad. Sci. U.S.A.* **116**, 7857–7866 (2019).
70. T. Ohn, N. Kedersha, T. Hickman, S. Tisdale, P. Anderson, A functional RNAi screen links O-GlcNAc modification of ribosomal proteins to stress granule and processing body assembly. *Nat. Cell Biol.* **10**, 1224–1231 (2008).
71. Q. Zeidan, Z. Wang, A. De Maio, G. W. Hart, O-GlcNAc cycling enzymes associate with the translational machinery and modify core ribosomal proteins. *Mol. Biol. Cell* **21**, 1922–1936 (2010).
72. K. E. Pyo *et al*., ULK1 O-GlcNAcylation is crucial for activating VPS34 via ATG14L during autophagy initiation. *Cell Rep.* **25**, 2878–2890.e4 (2018).
73. H.-B. Ruan *et al*., Calcium-dependent O-GlcNAc signaling drives liver autophagy in adaptation to starvation. *Genes Dev.* **31**, 1655–1665 (2017).
74. P. Wang, J. A. Hanover, Nutrient-driven O-GlcNAc cycling influences autophagic flux and neurodegenerative proteotoxicity. *Autophagy* **9**, 604–606 (2013).
75. E. P. Tan *et al*., Altering O-linked β-N-acetylglucosamine cycling disrupts mitochondrial function. *J. Biol. Chem.* **289**, 14719–14730 (2014).
76. W. Liu *et al*., PHF8 mediates histone H4 lysine 20 demethylation events involved in cell cycle progression. *Nature* **466**, 508–512 (2010).
77. J. Wysocka, M. P. Myers, C. D. Laherty, R. N. Eisenman, W. Herr, Human Sin3 deacetylase and trithorax-related Set1/Ash2 histone H3-K4 methyltransferase are tethered together selectively by the cell-proliferation factor HCF-1. *Genes Dev.* **17**, 896–911 (2003).
78. S. Minocha *et al*., Rapid recapitulation of nonalcoholic steatohepatitis upon loss of host cell factor 1 function in mouse hepatocytes. *Mol. Cell. Biol.* **39**, (2019).
79. T. M. Kristie, Y. Liang, J. L. Vogel, Control of α-herpesvirus IE gene expression by HCF-1 coupled chromatin modification activities. *Biochim. Biophys. Acta* **1799**, 257–265 (2010).
80. M. L. Hancock *et al*., Insulin receptor associates with promoters genome-wide and regulates gene expression. *Cell* **177**, 722–736.e22 (2019).
81. J. L. Vogel, T. M. Kristie, Site-specific proteolysis of the transcriptional coactivator HCF-1 can regulate its interaction with protein cofactors. *Proc. Natl. Acad. Sci. U.S.A.* **103**, 6817–6822 (2006).
82. L. Franco-Serrano *et al*., Multifunctional proteins: Involvement in human diseases and targets of current drugs. *Protein J.* **37**, 444–453 (2018).
83. G. M. Burslem, C. M. Crews, Proteolysis-targeting chimeras as therapeutics and tools for biological discovery. *Cell* **181**, 102–114 (2020).
84. H. M. Itkonen *et al*., *Inhibition of O-GlcNAc Transferase Renders Prostate Cancer Cells Dependent on CDK9* (Mol. Cancer Res. MCR, 2020), 10.1158/1541-7786.MCR-20-0339.
85. E. W. Deutsch *et al*., The ProteomeXchange Consortium in 2017: Supporting the cultural change in proteomics public data deposition. *Nucleic Acids Res.* **54**, D1100–D1106. Deposited 20 November 2020.
86. Y. Perez-Riverol *et al*., The PRIDE database and related tools and resources in 2019: Improving support for quantification data. *Nucleic Acids Res.* **47**, D442–D450. Deposited 20 November 2020.